A mm-Wave Frequency-Agile Quadrature Receiver for Atmospheric Sensing

Milad Frounchi, *Graduate Student Member, IEEE*, John D. Cressler, *Fellow, IEEE*

***Abstract*—In this work, we proposed a V-band frequency-agile quadrature receiver for atmospheric radiometry. The frontend Dicke switch is codesigned with the LNA to obtain a low noise figure and improve the radiometer resolution. Broadband and low-loss mm-wave quadrature signal generation techniques are explored to suppress the image signal by 40 dB and maintain a high dynamic range. High efficiency frequency multipliers are also studied to minimize the system power consumption. To enable on-chip calibration, the noise performance and long-term reliability of on-chip PN junctions were evaluated, and a calibration noise source is coupled to the front-end circuitry. These receiver blocks were integrated to form a high-performance radiometer, and the fabricated chip was characterized to evaluate its technology readiness level. Employing this integrated radiometer frontend can minimize the risk of space radiometry missions by reducing the payload size, weight, power consumption and cost (SWaP-C) and enable economical manufacturing of mm-wave radiometers for the constellations of Earth-observing CubeSats.**

***Index Terms*—Article submission, IEEE, IEEEtran, journal, LaTeX, paper, template, typesetting.**

I. Introduction

MICROWAVE remote sensing has uniquely contributed to the study of atmospheric dynamics and climatology. These remote sensing observations should be made from space to collect global-scale data. Spaceborne radiometers were traditionally hosted on large multi-instrument satellites, but the challenge of data continuity induced a paradigm shift towards very small satellites (e.g., CubeSats) in distributed constellations to achieve faster revisit rates. Fig. 1(a) shows a CubeSat-based radiometer, whose benefits are demonstrated by the recent development of prototypes, including MicroMAS [1], MiRaTA [2], and RACE [3]. However, most of these designs use off-the-shelf components with multiple chips/modules. An integrated frontend can significantly reduce the complexity of the space-grade packaging.

Atmospheric remote sensing is typically performed at the resonance frequencies of oxygen and water vapor. Fig. 1(b) shows a set of weighting functions of a temperature profile-meter, which can extract the atmospheric temperature by observing the microwave radiations of the atmosphere across V-band frequency range. The proposed radiometer shown in Fig. 1(c) is a single sideband receiver, and it consists of a single-pole double-throw (SPDT) switch, a low-noise-amplifier (LNA), an image-reject (IR) mixer, a frequency multiplier, and a calibration noise source. This frontend uses a sliding LO receiver architecture to eliminate the need for high-power broadband ADCs.

Manuscript received March 11, 2022. Milad Frounchi and John D. Cressler are with the School of Electrical and Computer Engineering, Georgia Institute of Technology, Atlanta, GA 30332 USA (e-mail: frounchi@gatech.edu; cressler@ece.gatech.edu)

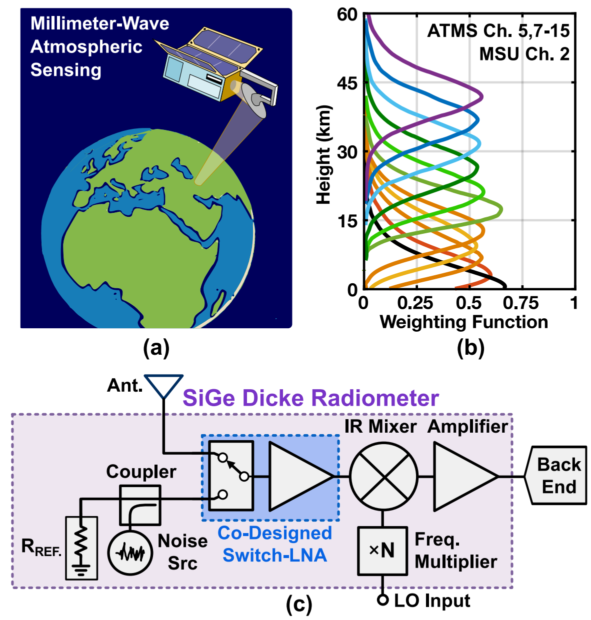

Fig. 1. a) CubeSat-based atmospheric sensing, b) weighting functions of a temperature profile-meter, and 3) block diagram of the propose receiver.

II. Circuit Design

Quantifying and predicting climatological changes in atmospheric temperature is a critical earth science need. However, these changes are in the order of 0.16 °C/decade, requiring highly accurate and stable radiometers with low noise figure (NF). We proposed a co-designed Dicke switch and low-noise amplifier (LNA) in [4] where the switch incorporates a transformer-based topology and it serves as the LNA input matching network, reducing the overall loss and NF.

To achieve a high image rejection ratio (IRR) in the mixer, we implemented a novel broadband low-loss quadrature signal generation network [5]. This idea is similar to cascading RC polyphase filters, and it is based on coupled-line couplers. Several stages can be cascaded to provide broadband balanced quadrature signals, and each stage has a low loss of 0.5 dB and improves the IRR by approximately 8 dB. A high IRR of 40 dB can be achieved without any calibration, tuning, or trimming [5]. The V-band LO signals were generated by a two-stage class C push-push frequency quadrupler.

Radiometers must be regularly calibrated with known noise sources to ensure accurate measurements. In modern radiometers, electronic calibration sources are often integrated into the receiver, in front of the LNA, to enable frequent in-situ calibration. The noise performance and the long-term reliability of several on-chip PN junctions are studied in [4],

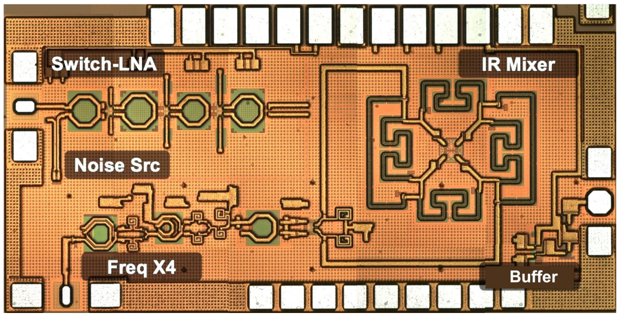

Fig. 2. Receiver micrograph occupying a die area of 1.8 mm^2.

and in this work, the noise source with highest excess noise ratio is coupled to the front-end circuitry to enable on-chip calibration. The long-term reliability of these noise sources was evaluated, and they were shown to be stable [4].

III. Measurement Results

The proposed integrated receiver was fabricated in a commercial 130-nm SiGe BiCMOS platform, as shown in Fig. 2. This chip occupies a die area of 1.8 mm^2 and it consumes a dc power of 45 mW. The S-parameters were measured using an Agilent E8361C network analyzer, and a Quinstar WR-15 noise source and an Agilent E4440A spectrum analyzer were used to measure NF. This NF measurement was performed independently for the LNA while the device temperature was set to 300, 150, 78, and 20 K. For conversion gain and IRR measurements, the RF and LO signals were provided by two Agilent signal generators (E8257D), and the IF signal was captured with an Agilent spectrum analyzer (E4440A). The measurements are performed with an external LO power of -5 dBm.

The simulated and the measured results are compared in Fig. 3, where the input port is matched with better than -15 dB reflection. A minimum NF of 4.5 dB was measured at room temperature and it decreases significantly as temperature decreases, achieving an average NF of 0.7 dB across 50–58 GHz at 20 K. The frontend gain is about 22 dB, and a record IRR of 60 dB is obtained at the desired band. The main difference between this IR mixer and the one presented in [5] is that the IF polyphase filter in this design is also drawn with a common-centroid layout, minimizing phase and amplitude mismatches. Such a high-performance receiver is a promising solution for CubeSat-based radiometry systems.

IV. Career Plan and Fellowship Impact

It is an honor to be one of the recipients of the IEEE Microwave Theory and Techniques Society (MTT-S) graduate fellowship award and to be recognized by a leading community in my professional field. This award has boosted my confidence and motivation to keep pursuing my research, and it also provided me an opportunity to attend the IMS 2021 and have close interactions with many colleagues in the field. Regarding future career, I am planning to work for industry to gain some experience, and hopefully return to academia after a couple of years, where I can contribute more to the microwave community.

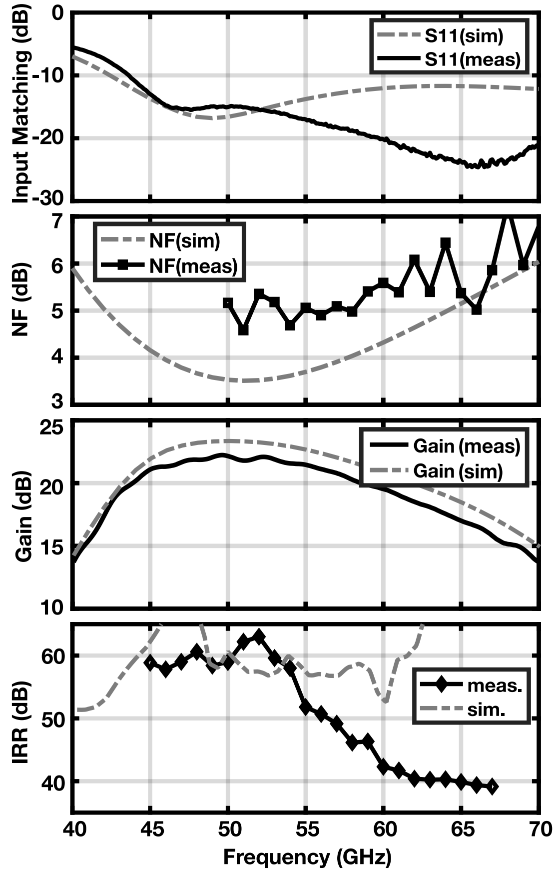

Fig. 3. Simulation and measurement results.

Acknowledgments

I would like to thank the MTT-S community for selecting me for the IEEE MTT-S Graduate Fellowship. I would also like to thank my advisor, Dr. John D. Cressler, for being always supportive and encouraging me along the way. Finally, I would like to thank Dr. Al Gasiewski for all the technical discussions on radiometry and remote-sensing challenges.

References

[1] W. J. Blackwell, “The MicroMAS and MiRaTA CubeSat Atmospheric Profiling Missions,” in IEEE MTT-S Int. Microw. Symp., Phoenix, AZ, 2015, pp. 1-3.

[2] W. J. Blackwell, “Technology Development for Small Satellite Microwave Atmospheric Remote Sensing,” in IEEE MTT-S Int. Microw. Symp., Honolulu, HI, 2017, pp. 222-225.

[3] B. Lim et al, “Development of the Radiometer Atmospheric CubeSat Experiment payload,” in IEEE IGARSS Int. Geosci. and Remote Sens. Symp., Melbourne, VIC, 2013, pp. 849-851.

[4] M. Frounchi et al, ”Millimeter-Wave SiGe Radiometer Front End With Transformer-Based Dicke Switch and On-Chip Calibration Noise Source,” in IEEE Journal of Solid-State Circuits, vol. 56, no. 5, pp. 1464-1474, May 2021.

[5] M. Frounchi et al, ”A Low-Loss Broadband Quadrature Signal Generation Network for High Image Rejection at Millimeter-Wave Frequencies,” in IEEE Transactions on Microwave Theory and Techniques, vol. 66, no. 12, pp. 5336-5346, Dec. 2018.